AFRL-AFOSR-UK-TR-2015-0008

Modelling ferroelectric nanoparticles in nematic liquid crystals (FERNANO)

Prof. Claudio Zannoni

DIPARTIMENTO DI CHIMICA FISICA ED INORGANICA
VIALE DEL RISORGIMENTO 4
BOLOGNA, 40136 ITALY

EOARD GRANT #FA8655-11-1-3046

Report Date: February 2015

Final Report from 1 September 2011 to 31 August 2014

Air Force Research Laboratory
Air Force Office of Scientific Research
European Office of Aerospace Research and Development
Unit 4515, APO AE 09421-4515

REPORT DOCUMENTATION PAGE

Form Approved OMB No. 0704-0188

1. REPORT DATE *(DD-MM-YYYY)*	2. REPORT TYPE	3. DATES COVERED *(From – To)*
26 February 2015	Final Report	1 September 2011 –31 August 2014

4. TITLE AND SUBTITLE

Modelling ferroelectric nanoparticles in nematic liquid crystals (FERNANO)

5a. CONTRACT NUMBER

5b. GRANT NUMBER

FA8655-11-1-3046

5c. PROGRAM ELEMENT NUMBER

61102F

6. AUTHOR(S)

Prof. Claudio Zannoni

5d. PROJECT NUMBER

5d. TASK NUMBER

5e. WORK UNIT NUMBER

7. PERFORMING ORGANIZATION NAME(S) AND ADDRESS(ES)

DIPARTIMENTO DI CHIMICA FISICA ED INORGANICA
VIALE DEL RISORGIMENTO 4
BOLOGNA, 40136 ITALY

8. PERFORMING ORGANIZATION REPORT NUMBER

N/A

9. SPONSORING/MONITORING AGENCY NAME(S) AND ADDRESS(ES)

EOARD
Unit 4515
APO AE 09421-4515

10. SPONSOR/MONITOR'S ACRONYM(S)

AFRL/AFOSR/IOE (EOARD)

11. SPONSOR/MONITOR'S REPORT NUMBER(S)

AFRL-AFOSR-UK-TR-2015-0008

12. DISTRIBUTION/AVAILABILITY STATEMENT

Distribution A: Approved for public release; distribution is unlimited.

13. SUPPLEMENTARY NOTES

14. ABSTRACT

The report provides the results of Monte Carlo computer simulation studies on systems of rod-like mesogens doped with nanoparticles. In particular, we have focused on the effects of nanoparticle shape (spherical, rod and disk–like), strength of the specific interactions between nanoparticles and between nanoparticles and mesogens (solvent affinity), polarity of the nanoparticles on phase behavior, long-range positional and orientational order and overall organization of these mixture systems.

The results clearly show that even a simple model based on a multi-site Gay–Berne potential and dipolar interaction can help to figure out the features which favors the enhancement of the LC order as well as the formation of nanoparticle aggregates.

In particular we found that doping a mesogenic system with nanoparticles of any shape has the overall effect of reducing both the orientational and positional order, with the most disordering effects observed for the embedded spherical nanoparticles.

The specific nanoparticle-solvent interaction has a significant influence in determining the aggregation/dispersion state of the dopant NP, anyway all the mixtures evidence a shift of the TNI temperature towards lower values, if compared with the pure system. The only exception is given by the mesogenic system doped with polar rod-shaped NP with very low solubility features, which essentially shows invariance of the ordering properties and of the relevant transition temperatures. This behavior is related to the formation of nanoparticles aggregates, each aggregate containing a large number (> 20) of nanoparticles, overall oriented along the mesophase director.

15. SUBJECT TERMS

EOARD, BaTiO3 FNP, ferroelectric nanoparticles, GB mesogens, modellimg of ferroelectric nanoparticles, Molecular Dynamics simulations, nematic liquid crystal, nematogen (5CB), tetragonal BaTiO3, tetragonal crystal

16. SECURITY CLASSIFICATION OF:			17. LIMITATION OF ABSTRACT	18, NUMBER OF PAGES	19a. NAME OF RESPONSIBLE PERSON
a. REPORT	b. ABSTRACT	c. THIS PAGE			John Gonglewski
UNCLAS	UNCLAS	UNCLAS	SAR	14	19b. TELEPHONE NUMBER *(Include area code)* +44 (0)1895 616007

Grant number: **FA8655-11-1-3046**

Title of Proposal: **Modelling ferroelectric nanoparticles in nematic liquid crystals (FERNANO)**

Principal Investigator: **Prof. Claudio Zannoni**

Period of Performance: **1 Sep 2011 - 31 Aug 2014**

Table of Contents

List of Figures

Fig.10: Average orientational order parameters $\langle P_2 \rangle_M$ and $\langle P_2 \rangle_N$ against the dimensionless temperature T^* for LC-NP dispersions within the low affinity regime (left panel) . Example of a nanoparticle aggregate for ε_s =2.0 at T*=1.3 (right panel).

Fig. 11: Mesogenic orientational order parameter $\langle P_2 \rangle$ against the dimensionless temperature T^* for polar LC/polar NP dispersions within the low affinity regime.

Fig.12: Local first rank, $\langle P_1 \rangle$, and second rank, $\langle P_2 \rangle$, orientational order parameters referred to nanoparticles against the temperature T^* for ε_s =2.0 and e_{NM} = 0.5 (left panel). Example of a nanoparticle aggregate at T*=1.3 (right panel).

Fig. 13: Examples of fits of EPR experimental spectra of a 1% w/w $BaTiO_3$ NPs in BL038 suspension. From top to bottom: sample in the nematic N phase, in the NI coexistence T interval, and in the I phase, respectively.

Fig. 14: Orientational order parameter $\langle P_2 \rangle$ (left) and tumbling rotational diffusion coefficient $D_\perp$ (right) of the spin probe in the BaTiO3 doped samples (1% - blue dots - and 0:5% dispersions - green squares) plotted versus the reduced temperature T* (= T/T_{NI}), compared to the pure LC (red triangles) behavior

Introduction

The addition of nanoparticles (NP)s and in particular of ferroelectric NPs to nematic liquid crystals has proved to be an important way of modifying the liquid crystal properties[1-8], particularly increasing the susceptivity to external electric fields without sensibly altering their optical properties, although their effect is still poorly understood.

In this project we carried out Monte Carlo computer simulation studies on mesogenic systems doped with nanoparticles, focusing on the effects on phase behavior, long-range positional and orientational order and overall organization of these mixture systems of

- nanoparticle shape (spherical, rod and disk–like)
- strength of the specific interactions between nanoparticles and between nanoparticles and mesogens (solvent affinity)
- polarity of the nanoparticles

Electron Paramagnetic Resonance (EPR) experiments have also performed on diluted suspensions of $BaTiO_3$ ferroelectric nanoparticles in the commercial LC mixture BL038 focusing in particular on the determination of Nematic to Isotropic (NI) transition temperature, and on the possible variation in the nematic director configuration, as well as on the local molecular order and dynamics.

Methods, Assumptions, and Procedures

The work can be divided in various sections aimed at atomistic (part 1) and coarse-grained (part 2) modeling of nanoparticles (NP) and at Monte Carlo (MC) simulations of dispersions of coarse – grained NPs of different shape (Part 2), affinity (Part 3), polarity (Part 4) and to experimental EPR investigations (Part 5).

Part 1) This first section essentially aimed at modeling at atomistic level a ferroelectric nanoparticle endowed with a partial charge on every atom as a cluster of spherical centers "decorated" with a reduced number of suitable charges[9].

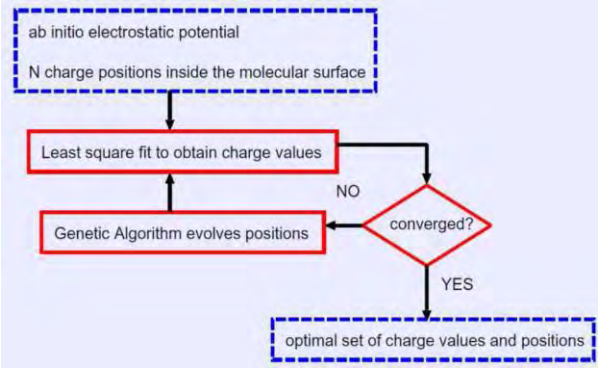

Fig. 1 Flow-chart of the charge reduction algorithm

A further simplification involved coarse graining the atomistic detailed NP. In practice we reduced the number of interaction centers by replacing each unit cell with a Lennard- Jones (LJ) spherical site.

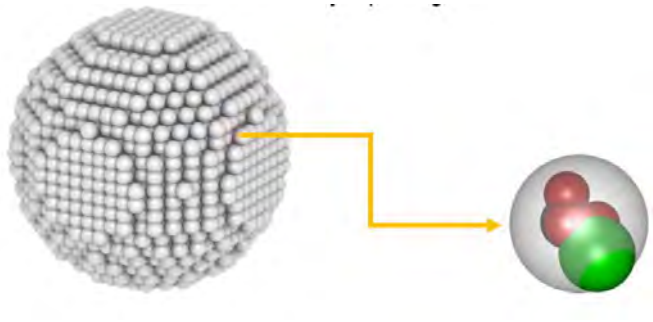

Fig.2: NP modeled as a collection of LJ spheres (number of spheres is 5375)

The reduced charges previously obtained can then be placed appropriately on a few of these spheres.

Part 2) In the second part of the project, we have modeled different nanoparticle-mesogen interactions, assuming the mesogens to be represented as soft rod–like Gay-Berne (GB) ellipsoids [10-13], and the nanoparticles as a closed packed cluster of identical Lennard–Jones (LJ) spheres [14], slightly overlapping and rigidly connected with each other and assembled so as to approximate the actual shape of the NP.
The total interaction between any pair of species, mesogenic (M) or nanoparticle (N), involves a summation over all the constituent sites, rodlike or spherical ones. Each pair of like (A=B) or unlike sites (A ≠ B), with labels i and j, interacts through a Gay–Berne potential:

$$U_{AB}^{GB}(\omega_i,\omega_j,\hat{\mathbf{r}}_{ij}) = 4\varepsilon_0 e_{AB}\varepsilon_{AB}^{\nu}(\omega_i,\omega_j)\varepsilon_{AB}^{\prime\mu}(\omega_i,\omega_j,\hat{\mathbf{r}}_{ij})\times$$
$$\left[\left(\frac{\sigma_c}{r_{ij}-\sigma_{AB}(\omega_i,\omega_j,\hat{\mathbf{r}}_{ij})+\sigma_c}\right)^{12}-\left(\frac{\sigma_c}{r_{ij}-\sigma_{AB}(\omega_i,\omega_j,\hat{\mathbf{r}}_{ij})+\sigma_c}\right)^{6}\right]$$

where A and B could be of M or N type.
We have until now modeled three different shapes, namely spherical, rod–like and disk–like [14], but an important point is that our approach is quite general and will allow to model more realistic NP shape similar to those obtained in the milling process used in the USAF partner lab of Dr. D. Evans.

r*

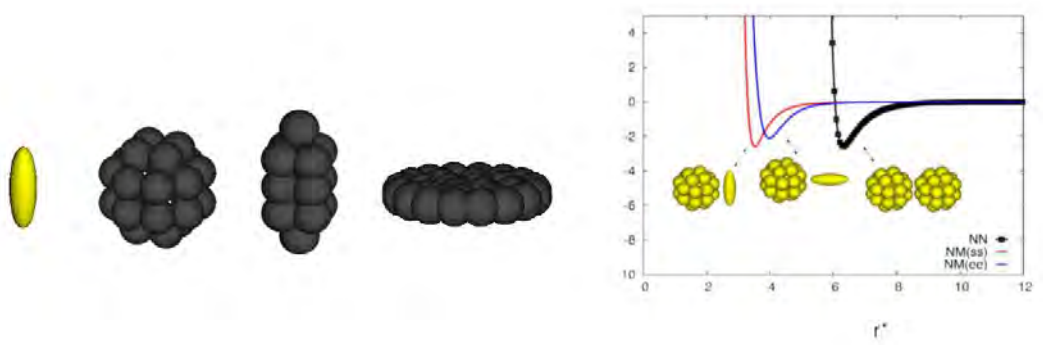

Fig. 3: Schematic drawings of the proposed models for mesogen and for differently shaped nanoparticles (left) and representative pair potential profile relative to the homogeneous NP-NP interaction (NN), as well as the NP-mesogen (NM) one for the spherical NP shape.

Part 3) To control the strength of the specific interactions, we introduced in the formula for the potential an affinity parameter e_{AB}, which rescales the amplitude of the single site-site pair energy.
We have considered two different values for e_{NM}, corresponding to weak or strong affinity regimes; for each value of $e_{NM,}$ we tested three value of ε_S, which acts as parameter controlling the nanoparticle–nanoparticle interaction:

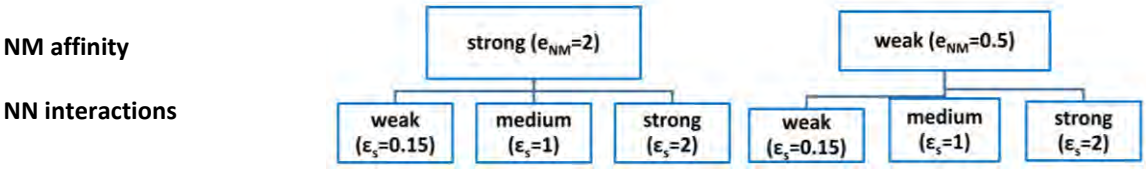

Part 4) The aim of this task is the study of the effects on the liquid crystalline phase associated to the presence of a longitudinal centered dipole moment embedded in the rod-like nanoparticle

Part 5) The modeling and computer simulation activity has been complemented by experimental work using EPR spectroscopy [15-17] to obtain data at molecular level on the order and fluidity of the NP dispersions in liquid crystals. These data, scarcely available, if at all, in the literature and precious to validate simulations and refining the NP models, are determined using a spin probe (in practice a stable nitroxide) dispersed at low concentration in the suspension to produce a spectrum sensitive to the fluid environment that is analyzed with techniques partly developed in the group.

Results and Discussion

Part 1) The atomistic modeling has shown the possibility of obtaining a good representation of the electrostatic potential around a $BaTiO_3$ NP. Starting from the $BaTiO_3$ atomic formal charges, and using a genetic algorithm developed in [9], we found a reduced number of charges, that reproduce the electrostatic field near the surface of the NP.

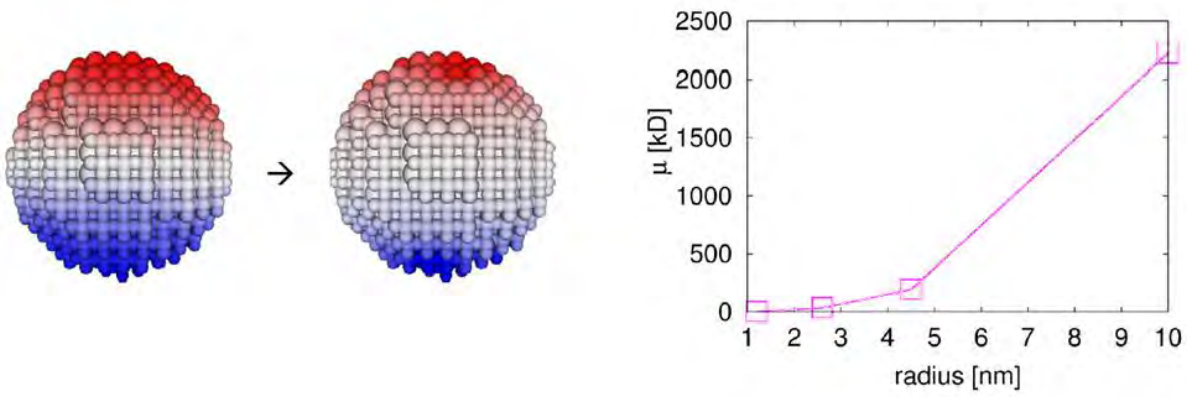

Fig. 4 Electrostatic potential generated by the full atomic charges, and by a reduced set of charges, for spherical nanoparticles carved from a tetragonal BaTiO3 mapped onto the NP surface. The color palette indicates potential level from negative (blue) to positive (red) (left panel) and NP dipole moment (kDebye) as a function of NP radius (right panel).

Part 2) Monte Carlo (MC) simulations have been first performed on pure mesogenic systems that will be considered as a reference for the dispersions with different embedded nanoparticles. We consider systems of N = 4000 GB rods in the isobaric-isothermal (NPT) ensemble using 3D periodic boundary conditions in a range of temperatures wide enough to observe both isotropic–nematic and nematic–smectic B transitions of the pure mesogen.
For each system, MC experiments were run in a cooling sequence starting from isotropic configurations. From the equilibrium configurations we computed the average values of the orientational order parameter $\langle P_2 \rangle = (3 \langle \cos^2 \beta \rangle - 1)/2$, where β is the angle between mesogen long axis and director. $\langle P_2 \rangle$ shows a steep increase at T*=1.7, corresponding to the first order isotropic–nematic transition, and a further jump at $T^* = 1.1$ denoting the nematic–smectic B transition (Fig. 5) .

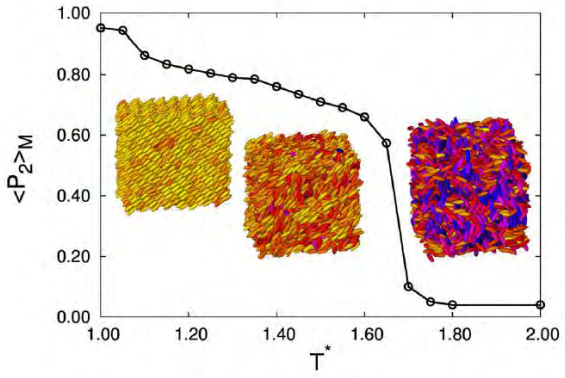

Fig. 5: Average orientational order parameter $\langle P_2 \rangle_M$ versus dimensionless temperature T for the pure mesogen with snapshots of the smectic ($T^* = 1.0$), nematic ($T^* = 1.5$) and isotropic ($T^* = 1.8$) phases: here the GB mesogens are color coded according to their orientation with respect to the phase director (yellow for parallel, blue for orthogonal).*

In a second set of investigations we performed simulations on sample mixtures of $N = N_M + N_N = 4000$ total particles with number of nanoparticles $N_N = 4,8,20$, corresponding to numerical concentration $c = N_N/N = 0.1\%, 0.2\%, 0.5\%$ respectively.

We considered three different shapes, namely spherical, rod–like and disk–like.
Compared to the pure mesogenic system (black line), a slight shift of the isotropic-nematic and nematic-smectic B transitions towards lower temperatures, with respect to the pure LC system, is evident for all the nanoparticle shapes, as shown by the plot of temperature dependence of the orientational order parameter in Figs. 6,7,8.
In addition, a general decrease of the LC orientational order is observed; this effect is particularly striking for the c=0.5% dispersions of spherical and disk-shaped embedded nanoparticles.

The local arrangement between nanoparticle-mesogen pairs indicates a weak planar anchoring with formation of LC orientational defects.

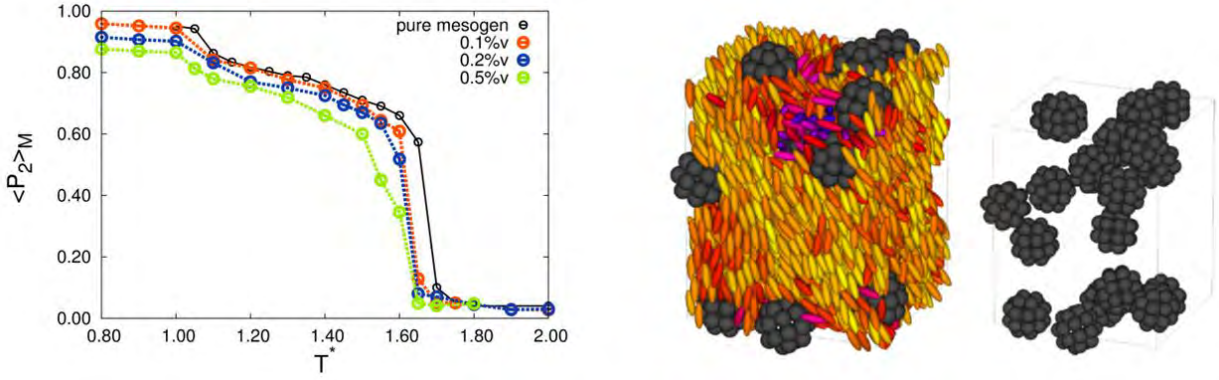

Fig. 6: Average orientational order parameter $\langle P_2 \rangle_M$ versus dimensionless temperature T for three LC/spherical NP dispersions, at increasing concentrations(left panel); A snapshot of an instantaneous configuration at T*= 1:5, c=0.5% showing a parallel weak anchoring (the multisite nanoparticle is represented in dark grey) (right panel.)*

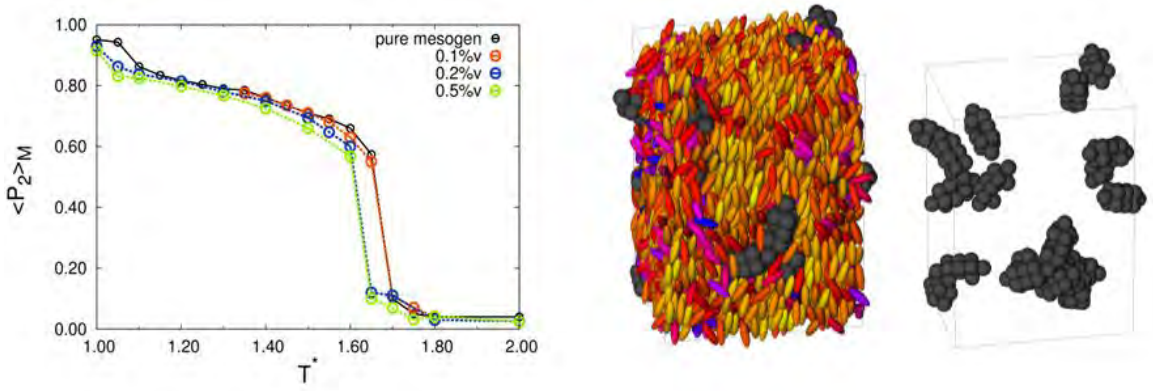

Fig. 7: Orientational order parameter $\langle \mathbf{P_2} \rangle_M$ against the dimensionless temperature T for three LC/rod-like NP dispersions, at increasing concentrations (left panel); A snapshot of an instantaneous configuration at T= 1:5; c = 0.5% showing a parallel weak anchoring (right panel).*

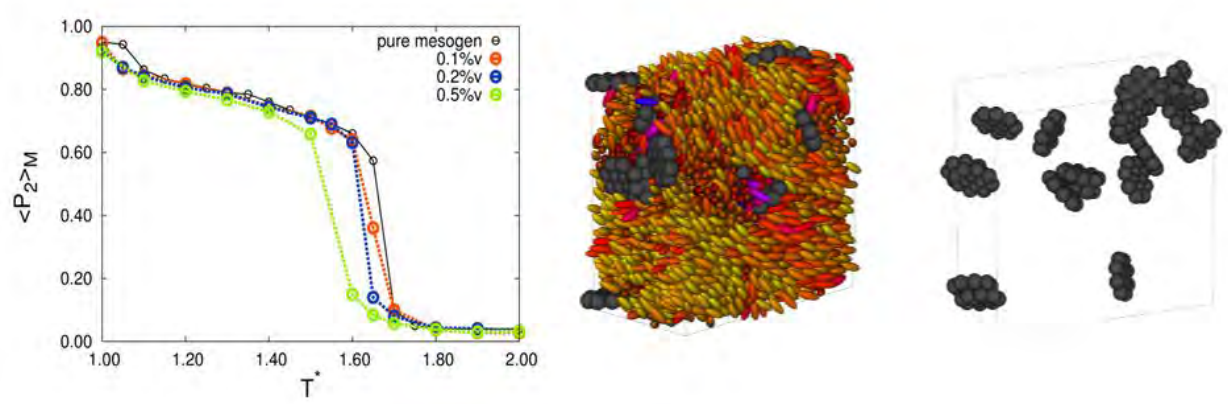

Fig. 8: Average orientational order parameter $\langle P_2 \rangle_M$ against the dimensionless temperature T for three LC/ disk-like NP dispersions, at increasing concentrations (left panel); A snapshot of an instantaneous configuration at T*= 1:5; c = 0.5% showing a parallel weak anchoring (right panel).*

Part 3) In the third section of the project we tried to assess the effect of the strength of the heterogeneous nanoparticle-mesogen affinity and of the homogeneous nanoparticle-nanoparticle interaction.

We performed simulations of mixtures formed by a constant number $N = N_M + N_N = 5000$ total particles where $N_M = 4975$ is the number of polar mesogenic molecules and $N_N = 25$ is the number of rod–like nanoparticles (corresponding to the solute fraction 0.5%) in two different cases: a) Strong NM affinity and NN interactions from weak to strong; b) Weak NM affinity and NN interaction from weak to strong.

a) Strong NM affinity and NN interactions from weak to strong ($e_{NM} = 2.0$, ε_S=0.15, 1, 2)
Embedding rod–like nanoparticles to the liquid crystal medium within a strong affinity regime results in a shift of the isotropic-nematic transition temperature towards lower values and in a small reduction of the mesogenic orientational order in comparison to the pure system; this effect is observed regardless the values of the homogeneous nanoparticle-nanoparticle interaction.

Focusing on the arrangement of nanoparticles, the simulations suggest that nanoparticles avoid to aggregate in clusters of significant size, irrespective from the values of ε_S, as apparent from the snapshots in Fig. 9.

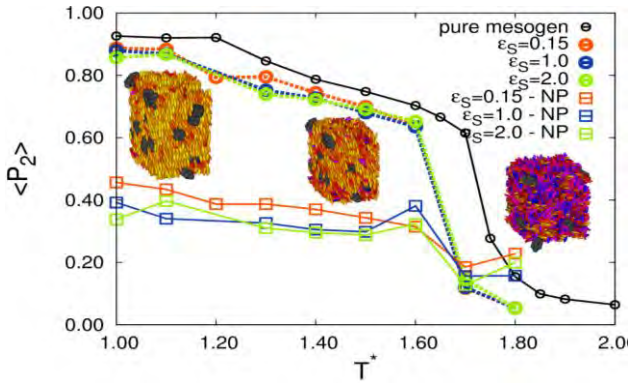

Fig. 9: Average orientational order parameters $\langle P_2 \rangle_M$ and $\langle P_2 \rangle_N$ against the dimensionless temperature T^* for LC-NP against the dimensionless temperature T^* within the strong affinity regime.

b) Weak NM affinity and NN interaction from weak to strong (e_{NM} = 0.5, ε_S=0.15, 1, 2)
The temperature dependence of the orientational order parameter for the dispersions in the weak affinity regime (shown in Fig. 10 for the three values of ε_S), still demonstrates a shift of the nematic-isotropic transition towards lower values.
The most striking difference between the two affinity regimes concerns the aggregation behavior: in fact, the overall effect of decreasing the nanoparticle-solvent affinity is to favor the formation of nanoparticles clusters, whose dimensions depend on the strength of nanoparticle–nanoparticle interactions. Analyzing a representative cluster (shown in Fig 12 for e_{NM} = 0.5, ε_S = 2.0), we observe that the NPs tend to maintain a random orientation instead of orienting along a preferred direction.

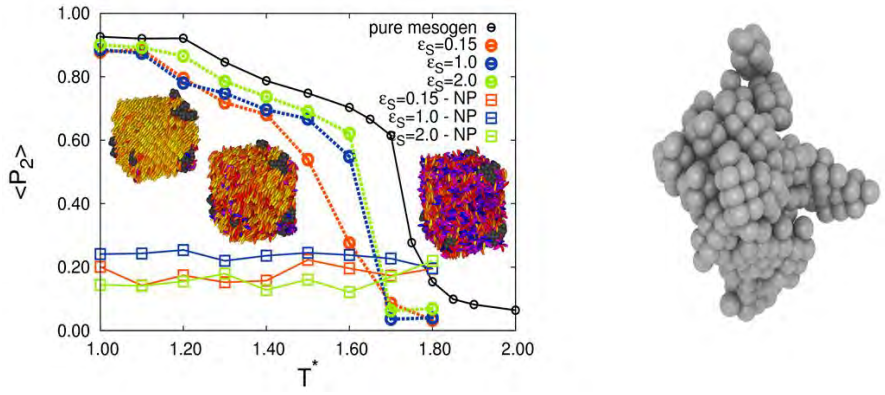

Fig.10: Average orientational order parameters $\langle P_2\rangle_M$ and $\langle P_2\rangle_N$ against the dimensionless temperature T^* for LC-NP dispersions within the low affinity regime (left panel). Example of a nanoparticle aggregate for ε_S =2.0 at T=1.3 (right panel).*

Part 4) In this section of the project we focused on the effects associated to the presence of a longitudinal centered dipole moment embedded in the rod-like nanoparticle on the liquid crystalline phase
We considered a sample mixture formed by constant number N = N_M +N_N = 5000 where N_M = 4975 is the number of polar GB molecules and N_N = 25 is the number of rod-like particle corresponding to the solute fraction 0.5%. We assumed a dipole strength (in dimensionless units) μ^*= 1 for the mesogen, and μ^*=20 for the nanoparticle. Interactions were calculated with the Reaction Field method, setting the external permittivity to ε_{RF} = 1.5 and cutoff R^*_c = 10.

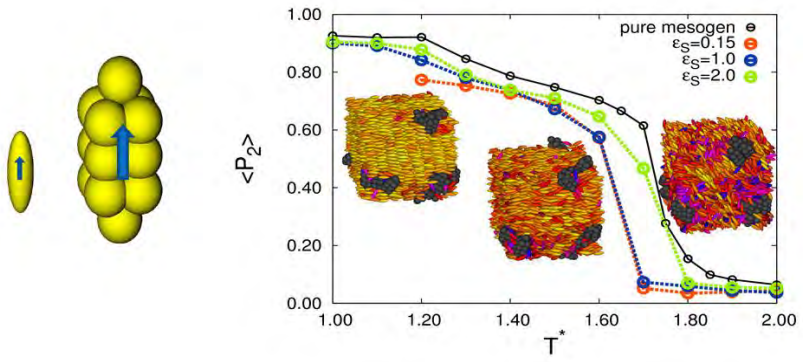

Fig. 11: Mesogenic orientational order parameter $\langle P_2\rangle$ against the dimensionless temperature T^* for polar LC/polar NP dispersions within the low affinity regime.

The analysis of the orientational order parameter plot against the temperature (Fig. 11) indicates behaviors comparable to the ones already detected for apolar NP when homogeneous NN interactions are small or medium (i.e. ε_s =0.15 and 1.0). Instead, and more interestingly, for the strongest homogeneous NN interaction (ε_s= 2:0), the Nematic-Isotropic transition remains unvaried with respect to the pure mesogenic system and overall both the orientational and positional order are substantially not affected by the introduction of nanoparticles.
Nanoparticles tend to form aggregates of large dimensions when NP-NP interaction is strong, i.e. ε_s= 2. Examining the clusters in detail, we notice that, differently from the apolar case, polar nanoparticles prefer to orient along the mesophase director (see Fig. 12), as strengthened by the behavior of second rank orientational order parameter, $\langle P_2 \rangle_{LOC}$, due to their embedded longitudinal dipole moments. On average the nanoparticles aggregate are almost apolar for any values of T*, as confirmed by the behavior of the local first rank order parameter $\langle P_1 \rangle_{LOC}$, as reported in Fig. 12.

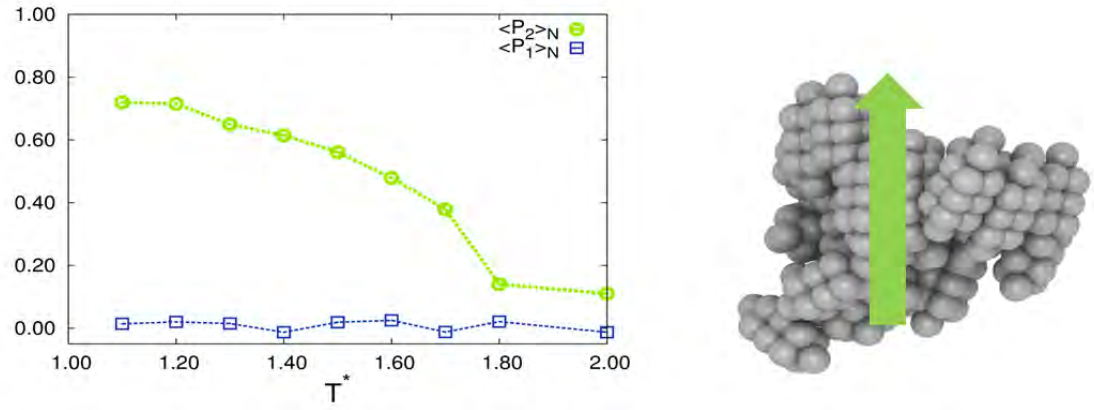

Fig.12: Local first rank, $\langle P_1 \rangle$, and second rank, $\langle P_2 \rangle$, orientational order parameters referred to nanoparticles against the temperature T^* for ε_s =2.0 and e_{NM} = 0.5 (left panel). Example of a nanoparticle aggregate at T=1.3 (right panel).*

Part 5) Experimental Results
The experimental work consisted in EPR measurements of suspensions of 0.5% and 1% w/w of 9 nm $BaTiO_3$ particles provided by Dr. D. Evans in the LC BL038 doped with the 3β-DOXYL-5α-cholestane spin probe (CSL), a reliable probe we have considerable experience with [15,16]. The measurements were carried out at controlled temperature T with a Bruker EMX spectrometer operating at X-band (9.5 GHz). Spectra were acquired on heating the samples from 294.2 K to 403.2 K. Annealing experiments were also performed to evaluate the possibility of enhancing the local order, by adding the NPs, heating the samples above their transition temperature (determined by the analysis of the heating run recorded spectra) and then cooling down gradually (using a 1 K/min rate) to a T in the N phase (303.2 K). A series of experimental spectra were analysed simultaneously with a global optimization method and using for each spectrum the fairly general “slow tumbling" rotational diffusional theory [17]. All the EPR spectra, independently of the concentration of the $BaTiO_3$ NPs in the LC, showed the typical features of spectra acquired in a low viscosity nematic LC, indicating the spin probe is moving in a host which is fluid and orientationally ordered at molecular level and. Fig.13 shows an example of EPR spectra of the investigated system consisting in BL038 LC doped with 1% harvested NPs. By a quick comparison between the central coexistence spectrum and the monophasic ones (N at the top and I at the bottom), it is quite evident that the lateral doubled peaks fall at the same field values as the I spectrum lateral peaks (the outermost ones), or as the N peaks (inner ones), confirming that the coexistence spectrum consists of a superimposition of a N and an I spectra.

All the recorded EPR spectra, independently of the concentration of the $BaTiO_3$ NPs in the LC, show the typical features of spectra acquired in a low viscosity nematic LC, indicating the spin probe is moving in a host which is fluid and endowed with a certain degree of order. Fig.13 shows an example of EPR spectra of the investigated system consisting in BL038 LC doped with 1% harvested NPs. By a quick comparison between the central coexistence spectrum and the monophasic ones (N at the top and I at the bottom), it is quite evident that the lateral doubled peaks fall at the same field values as the I spectrum lateral peaks (the outermost ones), or as the N peaks (inner ones), confirming that the coexistence spectrum consists of a superimposition of a N spectrum and an I one.

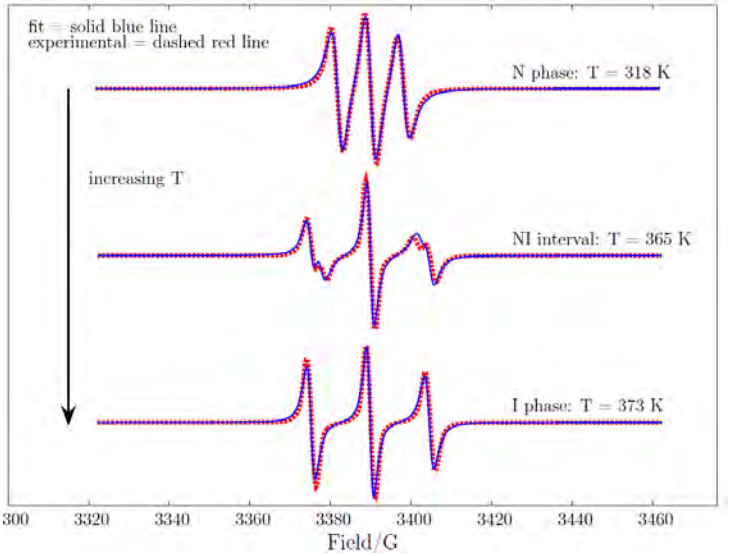

Fig. 13: Examples of fits of EPR experimental spectra of a 1% w/w $BaTiO_3$ NPs in BL038 suspension. From top to bottom: sample in the nematic N phase, in the NI coexistence T interval, and in the I phase, respectively.

Analysing the as already done with success in the case of similar LC complex systems [15,16] it was possible to derive from the experimental measures a value of orientational order $<P_2>$ and of tumbling rotational diffusion parameter $D_\perp$ for each temperature at which the spectra were acquired, and for each concentration of the ferroelectric nanoparticles (0%, 0.05%, and 1% w/w).

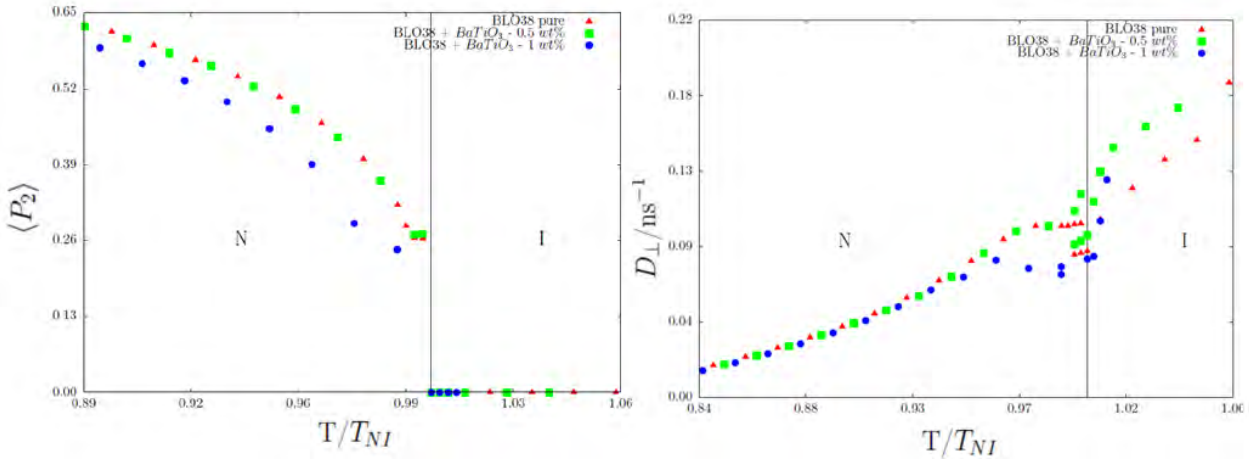

Fig. 14 : *Orientational order parameter $<P_2>$ (left) and tumbling rotational diffusion coefficient $D_\perp$ (right) of the spin probe in the $BaTiO_3$ doped samples (1% - blue dots - and 0:5% dispersions - green squares) plotted versus the reduced temperature T* (= T/T_{NI}), compared to the pure LC (red triangles) behavior*.

According to the figure above, the order parameter can be considered a universal function of T* only considering the lower concentration of barium titanate, while the behavior seems to change consistently when increasing its amount in the suspension: unfortunately, the effect is a decrease, and not an enhancement of the order, as reported in literature by other characterization techniques.

Moving to the dynamical behavior, the plot above confirms the results deduced by the analysis of the order parameter: while 0% and 0.5% samples share the same values (except for the T_{NI}) and the same trends, the higher concentration sample differs neatly, that is, the rotational diffusion abruptly increases in the I phase, the plot slope being steeper with respect to those of the other two samples.
In the nematic phase, on the contrary, the behavior appears unchanged independently of the sample, except for the region close to the T_{NI} , where again the 1% $BaTiO_3$ doped BL038 diverges experiencing a decrease.

Summary

We have reported the results of Monte Carlo computer simulation studies on systems of rod-like mesogens doped with nanoparticles. In particular, we have focused on the effects of nanoparticle shape (spherical, rod and disk–like), strength of the specific interactions between nanoparticles and between nanoparticles and mesogens (solvent affinity), polarity of the nanoparticles on phase behavior, long-range positional and orientational order and overall organization of these mixture systems.

The results clearly show that even a simple model based on a multi-site Gay–Berne potential and dipolar interaction can help to figure out the features which favors the enhancement of the LC order as well as the formation of nanoparticle aggregates.
In particular we found that doping a mesogenic system with nanoparticles of any shape has the overall effect of reducing both the orientational and positional order, with the most disordering effects observed for the embedded spherical nanoparticles.

The specific nanoparticle-solvent interaction has a significant influence in determining the aggregation/dispersion state of the dopant NP, anyway all the mixtures evidence a shift of the T_{NI} temperature towards lower values, if compared with the pure system. The only exception is given by the mesogenic system doped with polar rod-shaped NP with very low solubility features, which essentially shows invariance of the ordering properties and of the relevant transition temperatures. This behavior is related to the formation of nanoparticles aggregates, each aggregate containing a large number (> 20) of nanoparticles, overall oriented along the mesophase director.

Regarding the experimental part 0.5% and 1% w/w suspensions of milled and harvested 9 nm $BaTiO_3$ nanoparticles dispersed in the commercial liquid crystal mixture BL038 were investigated by EPR spin probe technique. The results can be summarized as follows: $\langle P_2 \rangle$ trend with respect to T* is universal only taking into account the pure LC and the 0.5% $BaTiO_3$ samples, while the 1% sample shows a different behavior, causing a reduction of the local order; which is accompanied by a reduction of the coexistence phase T range, which varies from 3 to 1 K; $D_{\perp}$ does not appear to be influenced by the presence of dopants in the N phase and displays a totally different slope in the I phase, only when the amount of ferroelectric nanoparticles is above 0.5% (w/w), showing a steep increase in the rotation speed.

References

[1] Y. Reznikov, O. Buchnev, O. Tereshchenko, V. Reshetnyak, A. Glushchenko and J. West, *Appl. Phys. Lett*., 82:1917 (2003).
[2] H.H. Liang, Y.Z. Xiao, F.J. Hsh, C. C. Wu and J.Y. Lee, *Liq. Cryst.,* 37:255 (2010)
[3] D.R. Evans, S.A. Basun, G. Cook, I.P. Pinkevych and V.Yu. Reshenyak, *Phys. Rev. B,* 84:174111 (2011)
[4] T. Hegmann, H. Qi and V.M. Marx, *J. Inorg. Organomet. Polym. Mat.,* 17:483 (2007)
[5] Q. Liu, Y. Cui, D. Gardner, X. Li, S. He and I.I. Smalyukh, *Nano Lett.,*10:1347 (2011)
[6] H. K. Bisoyi and S. Kumar, *Chem. Soc. Rev.*, 40:306 (2011)
[7] J. P. Lagerwall and G. Scalia, Curr. *Appl. Phys.,*12:1387 (2012)
[8] M. Mitov, C. Portet,C. Bourgerette, E. Snoeck and M. Verelst, *Nat.Mater.*,1:229 (2002).
[9] R. Berardi, L. Muccioli, S. Orlandi, M. Ricci, C. Zannoni *Chem. Phys. Lett.*, 0, 373-378 (2004)
[10] R. Berardi, L. Muccioli, S. Orlandi, M. Ricci and C. Zannoni, *J. Phys. Condens. Matter*, 20:463101 (2008)
[11] R. Berardi, A. Costantini, L. Muccioli, S. Orlandi, C. Zannoni , *J. Chem. Phys*.,126:044905 (2007)
[12] S. Orlandi, L. Muccioli, M. Ricci and C. Zannoni, *Soft Matter,* 5:4484(2009)
[13] S. Orlandi and C. Zannoni, *Mol. Cryst. Liq. Cryst.,* 573:1-9 (2013).
[14] E. Benini, S. Orlandi, D. Evans, V. Reshetnyak, I. Miglioli, M. Ricci, C. Zannoni, *to be published* (2015)
[15] A. Arcioni, C. Bacchiocchi, L.Grossi, A.Nicolini, C.Zannoni, *J. Phys. Chem. B*, 106, 9245-9251(2002)
[16] A. Arcioni, C. Bacchiocchi, I. Vecchi, G. Venditti, C. Zannoni, *Chem.Phys.Lett.,* 396, 433-441 (2004)
[17] J. H. Freed. Spin Labeling, Theory and Applications, chapter 3, Academic Press, NY, 1976

List of Symbols, Abbreviations, and Acronyms
NP:nanoparticle
LC: liquid crystal
GB: Gay-Berne